

Identification, Characterization, and Tissue Expression Pattern of Alternatively Spliced Transcript Variants of Mouse RARRES2 Gene

Kamila Kwiecien

Jagiellonian University

Pawel Majewski

Jagiellonian University

Maciej Bak

University of Basel

Piotr Brzoza

Jagiellonian University

Urszula Godlewska

Jagiellonian University

Izabella Skulimowska

Jagiellonian University

Joanna Cichy

Jagiellonian University

Mateusz Kwitniewski (✉ Mateusz.kwitniewski@uj.edu.pl)

Jagiellonian University

Research Article

Keywords: Chemerin , chemoattractant protein, retinoic acid receptor responder 2 (RARRES2), Chemerin bioactivity

Posted Date: April 1st, 2021

DOI: <https://doi.org/10.21203/rs.3.rs-371498/v1>

License: © ⓘ This work is licensed under a Creative Commons Attribution 4.0 International License.

[Read Full License](#)

Abstract

Chemerin is a chemoattractant protein with adipokine and antimicrobial properties encoded by the retinoic acid receptor responder 2 (*RARRES2*) gene. Chemerin bioactivity is largely dependent on carboxyl-terminal proteolytic processing that generates chemerin isoforms with the different chemotactic, regulatory and antimicrobial potential. While these mechanisms are relatively well known, a role of alternative splicing in generating isoform diversity remains obscure. Using rapid amplification of cDNA ends (RACE) PCR, we have identified novel transcript variant 4 of mouse *RARRES2* encoding mChem153K. Moreover, RT-QPCR results and analysis of publicly available RNA-seq datasets showed that different alternatively spliced variants of mouse *RARRES2* are present in mouse tissues, and their expression pattern was not affected by inflammatory nor infectious stimuli. Finally, we demonstrated that chemerin isoform mChem157S exhibits higher bactericidal but not chemotactic activity compared to mChem156S. Together, our findings highlight the importance of an alternative splicing in generation of chemerin isoforms diversity and activity.

Introduction

Protein isoforms can play important roles in various biological processes, like growth, differentiation or signal transduction. They can originate from separate genes, or single gene can code for multiple proteins due to the process called alternative mRNA splicing. Alternative polyadenylation, RNA editing, as well as post-translational modification may also generate the number of functionally distinct proteins. However, the alternative splicing of transcripts is one of the main sources of proteomic diversity in eukaryotes. Despite sharing a high degree of amino acid sequence homology, each isoform can have various, even opposite, biological roles.¹⁻³ Therefore, discovery of novel mRNA transcripts and protein isoforms may uncover new biological roles and functions of genes.⁴

Chemerin is a multifunctional chemoattractant, adipokine and antimicrobial agent capable of regulating different biological processes, including immune cell migration, adipogenesis, osteoblastogenesis, angiogenesis, glucose homeostasis and microbial growth.^{5,6} The gene encoding chemerin is known as retinoic acid receptor responder 2 (*RARRES2*), or as tazarotene-induced gene 2 (*TIG2*). Liver and adipose tissue are reported to be the major sites of chemerin production; nonetheless, *RARRES2* mRNA is detectable in many other tissues, including the adrenal glands, ovaries, pancreas, lungs, kidney, and skin.^{7,8} Chemerin-induced signalling is mediated predominantly through chemokine-like receptor 1 (CMKLR1), which is expressed by many cells including hepatocytes, adipocytes, keratinocytes, plasmacytoid dendritic cells (pDCs), or macrophages.^{7,9-13}

Chemerin is secreted as a pro-chemerin, functionally inert precursor protein referred to as hChem163S (human) or mChem162K (mouse), with number and capital letter referring to the terminal amino acid position and single amino acid code, respectively.¹⁴ Pro-chemerin can be converted to chemotactically active isoforms through posttranslational carboxyl-terminal processing by proteases belonging to the coagulation, fibrinolytic, and inflammatory cascades. The most active form of human chemerin,

hChem157S, can be produced by direct cleavage of six C-terminal amino acids by neutrophil elastase, or cathepsin G.¹⁵ Various proteolytic activities can generate other isoforms, including 152G, 153Q, 154F, 155A, 156F, and 158K, with low or no activity.^{15–18} Several murine chemerin isoforms have been characterized in a mouse model of obesity, mChem156S and mChem155F showed the highest biological activity.¹⁹

Mouse chemerin undergoes tissue-specific proteolytic cleavage similar to human chemerin.¹⁹ While mechanisms of proteolytic processing in generation of chemerin isoforms are relatively well described, a role of alternative splicing remains obscure. Mouse *RARRES2* gene is comprised of 6 exons and 5 introns. So far, three known (NM_001347168.1, NM_027852.3, NM_001347167.1) and one predicted (XM_011241467.3) protein-coding transcripts, encoding 162 and 163 aa protein, have been described.²⁰ The mChem162K is the major chemerin form in plasma.¹⁹ However, tissue expression profile and physiological role of mChem163K remains to be determined.

Generation of multiple chemerin isoforms is a key to control local, and context-specific bioactivity of this protein. Therefore, better understanding of mechanisms underlying diversity of chemerin isoforms is of particular importance. Here, we show that alternatively spliced variants of mouse *RARRES2* are present across different tissues and organs. Moreover, in addition to the variants encoding mChem163K and mChem162K, we have identified new transcript variant 4 encoding mChem153K. We demonstrate that inflammatory, and infectious conditions do not affect expression pattern of *RARRES2* splice variants. Furthermore, we determined chemotactic and antimicrobial activity of chemerin isoforms generated by an alternative splicing, and show that mChem157S exhibit higher bactericidal but not chemotactic activity compared to mChem156S. As such, we provide novel insights into the mechanisms that may contribute to the chemerin isoforms diversity and activity.

Results

Characterization of alternatively spliced transcript variants of *RARRES2*.

To identify transcript variants of mouse chemerin present in adult mouse tissues including liver and white adipose tissue (WAT), 3' and 5' RACE PCR were performed. We detected three transcript variants that have been already described. Mouse *RARRES2* variant 1 represents the longest transcript and encodes the longer isoform 1 (mChem163K) (Fig.1 A-B). *RARRES2* variant 2 uses an alternate in-frame splice site in the 3' coding region, compared to variant 1. This results in a shorter protein (isoform 2, mChem162K), compared to isoform 1. *RARRES2* variant 3 differs in the 5' UTR and uses an alternate in-frame splice site in the 3' coding region, compared to variant 1. Therefore, variants 2 and 3 encode mChem162K. In addition to the previously reported variants 1, 2 and 3, we have identified the novel variant 4, generated by an alternate in-frame splice site in the 3' coding region (Fig. 1A-B). This variant 4 is composed of exons 1

to 6 (Fig. 1A). However, exon 5 lacks 27 bp fragment. The transcript variant 4 of mouse *RARRES2* was not predicted nor annotated by Ensembl²¹ and RefSeq²².

The chemerin protein isoforms, encoded by transcript variants 1 to 4, were aligned (Fig.1C). *RARRES2* transcript variant 2 and 3 encode mChem162K which is the major chemerin form in plasma.¹⁹ Splice variant 1 codes for chemerin mChem163K that has one extra amino acid, glutamine, at position 128. Interestingly, newly discovered mChem153K, encoded by the transcript variant 4, is devoid of 10 amino acids 128-137 compared to mChem163K. All the changes in amino-acid sequence of mouse pro-chemerin are linked to exon 5.

Expression pattern of *RARRES2* splice variants across different tissues and experimental conditions.

Given the multiple existing alternatively spliced transcript variants, we next assessed in which tissues they are present and whether they were differentially expressed. To do so, we analyzed publicly available results of RNA-seq experiments or performed standard RT-QPCR.

Using VastDB²³, an atlas of alternative splicing profiles and functional associations in vertebrate cell and tissue types, we quantified transcript variants encoding for mChem162K and mChem163K but not mChem153K since transcript variant 4 is not included in the VastDB. The analysis revealed dominance of transcript variant 2 and 3 (mChem162K) in all investigated tissues with an average percent pliced in score (PSI) at around 68,5 (Fig. 2A). However, transcript encoding mChem163K accounted for up to 42% in cerebellum or pancreas. These results were corroborated by the RNA-Seq findings (Fig. 2B). In contrast, *RARRES2* transcript 4, encoding mChem153K, is rare and showed the PSI score up to 1.5 (Fig. 2A). The expression pattern of *RARRES2* splice variants was not changed by high-fat diet, viral, bacterial nor parasite infections. There were no statistically important differences between control and treatment groups. However, the levels of newly discovered *RARRES2* variant 4 tend to increase in kidney and skin after high-fat diet and *S. aureus* infection, respectively.

In line with the analysis of publicly available RNA-seq databases, RT-QPCR experiments confirmed that *RARRES2* variant 4 is rare with the highest levels found in heart (Fig. 3A). The relative incidence values (RIV)²⁴ of the variant 4 may vary from ~0,31% in liver up to ~3,4% in kidneys and seminal vesicles (Fig. 3B).

We have shown previously that acute-phase cytokines, interleukin 1b (IL-1 β) and oncostatin M (OSM), regulate chemerin expression in mouse adipocytes and human 3D skin cultures.^{7,25} Therefore, we next analyzed if these cytokines can affect the balance between newly discovered *RARRES2* transcript variant 4 and others splice variants in mouse tissues. The transcript ratio remained stable in all investigated mouse tissues, and there were no statistically significant differences between PBS and cytokine treated animals (Fig. 3C).

Expression of *RARRES2* protein isoforms in *E. coli* and HEK293 cells.

To determine the physiological role of mouse chemerin isoforms we set up production of full-length protein variants (mChem163K, mChem162K, mChem153K), and variants lacking 6 aa at C-terminus (mChem157S, mChem156S, mChem147S). To do so, we employed *E. coli* and previously established protocols used to produce human recombinant chemerin.²⁶ We were able to produce and purify mChem163K and mChem162K and their derivatives, but we could not purify mChem153K. This include purification on NI-sepharose, ion exchange chromatography purification (MonoSP and MonoQ sepharose), Ni-sepharose based purification in denaturing or semi-denaturing conditions, construction of expression vector coding for mChem153K containing two His-tag sequences at the N and C terminus, various protein expression strains of *E. coli* (BL21, ArcticExpress, Rosetta). However, western blotting analysis of a supernatant fraction from *E. coli* culture using an anti-His tag antibody revealed the presence of mChem153K band (Fig. 4A). To prove that *RARRES2* splice variant 4 can be translated into a protein in eucaryotic cells we transfected HEK293 cells with different chemerin constructs. Indeed, we detected mChem153K in cell lysates (Fig. 4B) but not supernatants (data not shown). Interestingly, the chemerin band was only present for protein with signal peptide and His-tag located at the C-terminus. Schematic representation of chemerin isoforms used in this study is shown on Fig. 4C.

Chemerin isoform mChem157S shows higher bactericidal but not chemotactic activity compared with mChem156S.

We hypothesized that changes in amino acid sequence of chemerin may affect its biological functions including chemotactic and bactericidal activity. Therefore, we performed transwell cell migration assay and antimicrobial microdilution assay (MDA) using chemerin responsive CMKLR1⁺ cells and *E. coli* HB101, respectively, and bioactive chemerin isoforms lacking six terminal aa, rmChemHis-157S and rmChemHis-156S. Bioactive chemerin isoform mChemHis-157S showed higher potency against *E. coli* HB101 by MDA assay compared with mChem156S (Fig. 5A). PBS and human (hu) or mouse (m) chemerin derived peptide p4 were used as a negative and positive controls, respectively; In contrast, there were no statistically significant differences in chemerin isoform-mediated chemotactic activity by transwell migration assay (Fig. 5B). Experiments were performed using at least two different chemerin production batches.

Discussion

Our knowledge of the post-translational modifications of chemerin that generate a variety of protein isoforms has increased significantly in the last two decades. However, these studies focused mainly on the proteolytic processing of human (hChem163S) or mouse pro-chemerin (mChem162K) by extracellular proteases.^{15,16,19,27,28}; Alternative splicing is a key factor increasing cellular and functional complexity.

Nevertheless, it remains obscure how an alternative splicing of *RARRES2* contribute to the isoforms diversity despite identification of at least three transcripts variants of murine chemerin encoding two different protein isoforms.²²

In this study, we have described, for the first time, transcript variant 4 of mouse *RARRES2* coding for 153 aa chemerin isoform 3 (mChem153K). mChem153K lacks 10 aa at the position 128–137 compared to isoform 1 (mChem163K). This modification may significantly affect protein structure since it removes cysteine residue involved in the formation of one out of three intrachain disulfide bonds.¹⁴ Therefore, conformational changes could be the reason why all the Chem153K purification procedures have failed. However, we have shown that mChem153K can be translated into protein since it was detectable in a supernatant fraction from *E. coli* culture and HEK293 lysates; Our *in silico* and *in vivo* studies have revealed that *RARRES2* transcript variant 4 accounts for a small fraction of other splice variants under physiological conditions. The average percentage for all investigated mouse tissues was 0,55 % and 1,31 % for RNA-seq and real time RT-PCR studies, respectively.

One common outcome of alternative splicing is downregulation of the function of a gene by the production of non-functional isoforms of the active gene product. This can be achieved by the alteration of functional domains of the protein.²⁹ Nonetheless, all the detected *RARRES2* transcript variants are generated by an alternate in-frame splice site in the 3' coding region of exon 5 or differs in the 5' UTR (variant 3). These modifications do not affect the C-terminal region of chemerin which is crucial for its bioactivity.⁵

Alternative transcripts are very often differentially expressed between cells or tissues and display different functions.^{30–32} Moreover, changes in alternative splicing events can be associated with exposure to different stimuli.³³ Altered chemerin expression may be of relevance in the context of pathological conditions like obesity, cancer, and inflammation.^{10,27,34–36} Chemerin expression is regulated by a variety of inflammatory and metabolic mediators in a manner dependent on cell type.^{25,37} We previously showed that IL-1 β and OSM upregulated chemerin expression in human skin cultures⁷, and mouse adipocytes²⁵. Moreover, bacteria, like *S. aureus*, upregulate chemerin levels in models of human epidermis and mouse skin.⁷ Skin transcriptome analyses of antimicrobial peptides differentially regulated following skin infection with *C. acnes* or *Leishmania braziliensis*, revealed elevated levels of *RARRES2* transcript.³⁸ Here, our study showed that splicing pattern of *RARRES2* mRNA was not altered by high-fat diet, bacterial, viral or parasite infection nor cytokine treatment in different mouse organs. Therefore, these factors are not the major determinants for splice site selection.

We also asked if there were any differences in antimicrobial or chemotactic activity between biologically active chemerin isoforms mChem157S and mChem156S, since they differ only by a single amino acid, glutamine, at position 128. This change does not affect directly antimicrobial region (p4) of chemerin, localized in the middle of the protein sequence (position 66–85 or 68–87 for human and mouse chemerin, respectively).⁶ Chemerin isoform mChem157S exhibited increased antibacterial activity

compared to mChem156S. In contrast, we did not find any changes in chemotactic activity. It is not clear how single amino acid can affect chemerin structure and functions. As is the case for chemoattractant activity, the inhibitory C-terminal peptide present in the pro-chemerin must be removed for full antibacterial effects. It was hypothesized that removal of inhibitory peptide enables structural accessibility of chemerin antimicrobial domain, and/or a release of internal antimicrobial peptide.²⁶

While four transcript variants of mouse *RARRES2* encoding three protein isoforms are known, there is only one confirmed splice variant of human *RARRES2* (NM_002889.4). This variant is translated into hChem163S precursor protein.²⁰ Interestingly, one predicted transcript (XM_017012491.1), encoding 132 aa peptide (isoform X1), is annotated in the NCBI database. Amino acid sequence of the C-terminal region of chemerin differs significantly between hChem163S and isoform X1. However, to date, such transcript variant has not been detected yet in human tissues.

In summary, our studies reveal novel insights into the mechanisms accounting for chemerin isoforms diversity. For the first time, we report the identification of rare transcript variant 4 of mouse *RARRES2*, encoding mChem153K (isoform 3). *RARRES2* transcript variants from 1 to 4 were present in all investigated mouse tissues, and variants encoding chemerin isoform mChem162K are the most abundant. Our research showed that splicing pattern of *RARRES2* mRNA was not altered by high-fat diet, bacterial, viral or parasite infection nor pro-inflammatory cytokine treatment. Chemerin isoform mChem157S showed higher antimicrobial but not chemotactic activity compared to mChem156S. These findings provide a basis for further investigations of the role of alternative splicing on chemerin functions.

Methods

Materials

If not stated differently, all chemicals were purchased from Sigma-Aldrich (St. Louis, MO, USA). Dulbecco's Modified Eagle medium (DMEM), and phosphate-buffered saline (PBS) buffer were purchased from PAN Biotech (Aidenbach, Germany). FBS was purchased from Gibco Laboratories (Gaithersburg, MD, USA). Mouse recombinant IL-1 β , OSM, mouse chemerin 156S, and human chemerin 157S were purchased from R&D Systems (Minneapolis, MN, USA). Chemerin-derived peptide p4 was chemically synthesized by ChinaPeptide (Shanghai, China) at $\geq 95\%$ purity.

Animal studies

Male eight- to 12-week-old C57BL/6 mice were used for these investigations. The mice were maintained under specific pathogen-free conditions at the Faculty of Biochemistry, Biophysics, and Biotechnology of Jagiellonian University animal care facility. IL-1 β and OSM were injected intraperitoneally at doses of 10 $\mu\text{g}/\text{kg}$ BW and 160 $\mu\text{g}/\text{kg}$ BW, respectively as previously described.²⁵ After 48 h, different tissues were

isolated and subjected to RT-QPCR analysis. All experimental procedures were approved by the First Local Ethical Committee on Animal Testing at the Jagiellonian University in Krakow, Poland (permit no. 41/2014), in accordance with the ARRIVE guidelines and the Guidelines for Animal Care and Treatment of the European Community. The mice were sacrificed by an overdose of anesthesia (a mixture of ketamine and xylazine), followed by cervical dislocation.

Rapid amplification of cDNA ends (RACE)

Total RNA was extracted as described by Chomczynski and Sacchi³⁹ and converted to complementary DNA using NxGen M-MuLV reverse transcriptase (Lucigen Corporation, Middleton, WI, USA) with random primers (Promega Corporation, Madison, WI, USA) and oligo dT (Genomed, Warsaw, Poland). 3' and 5' RACE PCR were performed with the 3' or 5' RACE System kit (Invitrogen, USA) according to the manufacturer protocol. The following *RARRES2* specific primers were used: 5'-GTGTGGACAGAGCTGAAGAAGTGCTCTTC (3' RACE) and 5'-CTGGAGAAGGCAAAGTGTCCAGGTAGGAAGTAG (5' RACE). RACE PCR products of interest were separated by agarose gel electrophoresis, excised from the gel, isolated using Gel-Out Concentrator (A&A Biotechnology, Poland), and ligated into pTZ57/RT vector using InsTAclone PCR Cloning Kit (Thermo Scientific, USA) followed by heat shock transformation of plasmid into chemically competent Top10 *E. coli*. Selected bacterial colonies were subjected to colony PCR using standard M13 primers. Plasmid DNA was recovered from positive clones using GeneJET Plasmid Miniprep Kit (Thermo Scientific, USA), and sequenced (Genomed, Poland). Results were analysed using SnapGene Viewer (GSL Biotech LLC, USA).

RT-QPCR and quantification of *RARRES2* splice variants

Total RNA was extracted with the Total RNA Zol-Out Kit (A&A Biotechnology, Gdynia, Poland) and converted to complementary DNA using NxGen M-MuLV reverse transcriptase (Lucigen Corporation, Middleton, WI, USA) with random primers (Promega Corporation, Madison, WI, USA). Real-time PCR was performed on the CFX96 thermocycler (Bio-Rad Laboratories, Hercules, CA, USA) using SYBR Green I containing universal PCR master mix (A&A Biotechnology, Gdynia, Poland) and the following mice specific primers: chemerin_all_variants (5'-CTTCTCCCGTTTGGTTTGATTG, 5'-TACAGGTGGCTCTGGAGGAGTTC), mChem162K (5' – CCTCAGGAGTTGCAATGCATTAAGAT, 5' -GTACAGGGAGTAAGGTGAAGTCTGT), mChem153K (5'- CAATCAAACCAAACGGGAGAAGGC, 5'-CGCCAGCCTGTGCTATCTGAG), cyclophilin A (5'- AGCATACAGGTCTGGCATCTTGT, 5'-CAAAGACCACATGCTTGCCATCCA), b-actin (5'-CCTTCTTGGGTATGGAATCCTG, 5'-TGGCATAGAGGTCTTTACGGA), GAPDH (5'-TGTGTCCGTCGTGGATCTGA, 5'-TTGCTGTTGAAGTCGCAGGAG). Expression stabilities of commonly used reference genes were analyzed as described previously.²⁵ Relative gene expression normalized to the geometric mean of these housekeeping genes was calculated using the $2^{-\Delta\Delta CT}$ method.⁴⁰ Relative Incidence of Variant (RIV) was

obtained with the method described by Londoño et al.²⁴, PCR efficiencies of primer sets were calculated with CFX Maestro Software (Bio-Rad) using pcDNA3.1 plasmids encoding mChem162K and mChem153K as a template

Alternative splicing analyses from RNA-Seq datasets

Information about *RARRES2* expression level in distinct tissues and cell lines as well as isoform quantification were acquired from VastDB.²³ To assess isoform ratios in publicly available RNA-Seq datasets we calculated Percent Spliced In (PSI) scores with vast-tools.²³ Notably, we analyzed NCBI:GEO datasets which investigate the molecular effects of high-fat diet: GSE76133, GSE75984 and GSE117249 as well as records related to transcriptional changes upon distinct infections: *Staphylococcus aureus* (GSE108718), *Toxoplasma gondii* (GSE119855) and influenza virus (GSE114232). Differential splicing analyses were carried out with vast-tool's module diff.

Plasmid construction

The pcDNA3.1(+) (ThermoFisherScientific, USA) and pNIC28-Bsa4(Addgene, LGC Standards, UK) plasmids, encoding mouse full-length chemerin variants mChem163K, mChem162K, mChem153K and chemerin variants mChem157S, mChem156S, mChem147S lacking 6 aa at C-terminus, were generated. Briefly, the expression plasmid insert was generated from mouse liver cDNA using Phusion High-Fidelity DNA Polymerase (ThermoFisherScientific, USA) and a primer set flanking *RARRES2* CDS with an overhang sequence complementary to plasmid fragment containing *Eco32I* restriction site (5'-TGTGGTGGAAATTCTGCAGATATGAAGTGCTTGCTGATC, 5'-CGGCCGCCACTGTGCTGGATTTATTTGGTTCTCAGGGC). In order to linearize the vector, the pcDNA3.1(+) plasmid was digested with *Eco32I*. Linearized vector and amplified insert were then assembled using NEBuilder HiFi DNA Assembly Master Mix (New England BioLabs, USA) and transformed into competent Top10 *E. coli*. Bacterial colonies were PCR-tested using universal T7/BGH primers and positive plasmids were sequenced in order to check for unintentional mutations. The following plasmids were generated: pcDNA-mChem163K, pcDNA-mChem157S, pcDNA-mChem162K, and pcDNA-mChem156S. In order to generate pcDNA-mChem153K and pcDNA-mChem147S, pcDNA-mChem162K/pcDNA-mChem156S plasmids were used as a template for overlap-extension PCR⁴¹ using Phusion Polymerase and primer set flanking 5' end of exon 5 with an inner fragment lacking specific sequence (5'-AAGCAAGGGCCTCAGATAGCACAGGCTGGCGAAGA, 5'-GCCAGCCTGTGCTATCTGAGGCCCTTGCTTCAGAA). The mixture was then digested with *DpnI* and transformed into Top10 *E. coli*, followed by identification of positive colonies and reamplifying and purification of plasmid DNA.

Then, pcDNA3vectors were used as a template to generate pNIC28-Bsa4 plasmids encoding different isoforms of chemerin (mChem163K, mChem162K, mChem153K, mChem157S, mChem156S,

mChem147S). The following starters: 5'-GCACCATCATCATCATCATTCTTCTGGTGAGCCCGAACTCAGCGAGACC, 5'-CACAATTCAGAAAATATCATAATATCTCATTTCCTACTATTTGGTTCTCAGGGCCCTGGAGAAG were designed to be complementary to a specific site of the target expression vector pNIC28-Bsa4. The PCR products were cloned into pNIC28-Bsa4 expression vector at a site preceded by the sequence coding for hexahistidine tag, using the overlap-extension PCR method. All constructs lacked the native chemerin signal peptide. The identity of the created pNIC28-Bsa4 constructs was verified by sequencing (Genomed, Warsaw, Poland).

Expression of mouse chemerins in HEK293 cells and western blot

HEK293 cells were grown in DMEM medium supplemented with 10% FBS and gentamycin (50 µg/mL). Cells were seeded at a density of 1.5×10^4 cells in a 24-well culture plate and, 24 h later. Then, the cells were transfected with the pcDNA plasmids described above using ViaFect transfection reagent (Promega Corporation, Madison, WI, USA) in accordance with the producers instructions. Transiently transfected cells were RIPA-lysed after 48h and used for Western Blot analysis. Proteins were electrophoretically separated on a SDS-polyacrylamide gel and wet-transferred onto PVDF membrane (Bio-Rad), followed by blocking with 5% skim milk (Merck). His-tagged chemerin isoforms were detected using anti-His tag antibodies (ab15149, Abcam, Cambridge, MA). Chemiluminescent detection was carried out using WesternBright ECL (Advansta) and ChemiDoc MP imaging system (Bio-Rad).

Production and purification of mouse chemerin isoforms in *E. coli*

Chemerin isoforms were expressed using *E. coli* strain NiCo21(DE3) (New England Biolabs, MA, USA) transformed with plasmids described above. Bacteria were precultured in 37°C in LB medium until culture density reached OD600 value between 0,6-0,8. Protein expression was induced by addition of IPTG to a final concentration of 1mM and carried out overnight in 18°C. After centrifugation the bacterial pellet was dissolved in PBS with 1mM EDTA and cOmplete protease inhibitor cocktail (Roche), and sonicated. After sonication samples were centrifuged (40000g, 20min, 4°C) and pellets were resuspended in denaturing buffer (6M GuHCl, 50mM NaCl, 50mM TRIS, pH8). After centrifugation (12000g, 12min, 4°C) supernatants were 100-fold diluted in renaturation buffer (0,5M GuHCl, 0,4M Sucrose, 0,1M TRIS, 1mM GSH, 0,1mM GSSG, pH8). Any precipitate was removed by centrifugation, and the protein solutions were concentrated using Amicon Ultra Centrifugal Filters (Merck). Concentrated solutions were 10-fold diluted in dilution buffer (0,1M TRIS, 0,1M Sucrose, 1mM GSH, 0,1mM GSSG, pH 8). Any precipitate was removed from solution by centrifugation. Proteins were purified from solution by incubation with Ni-Sepharose 6 Fast Flow (GE Healthcare, Uppsala, Sweden), washed on column in wash buffer (0,1M TRIS, 1mM GSH, 0,1mM GSSG, pH 8), then eluted with 500 mM imidazole in wash buffer. mChem163K and mChem162K

protein samples were dialyzed against buffer A (25mM TRIS, 25mM NaCl, pH 7,6). Any precipitates were removed by centrifugation. Protein samples were loaded on Q-Sepharose Fast Flow columns (GE Healthcare, Uppsala, Sweden). Elution fractions containing increasing concentrations of NaCl were collected and analysed by SDS-PAGE electrophoresis and coomassie blue staining. Fractions of low NaCl concentration were pooled, concentrated on Amicon Ultra Centrifugal Filters (Merck), and then dialyzed against PBS. Protein samples were routinely >90% pure as assessed by SDS-PAGE and Coomassie Blue staining. The concentration of chemerin was determined by measuring the absorbance at 280 nm using NanoDrop ND-1000 spectrophotometer (ThermoFisherScientific, USA), and bicinchoninic acid (BCA) assay (ThermoFisherScientific, USA). Chemerin activity profiling between batches was evaluated by *in vitro* transwell assay using CMKLR1 expressing L1.2 cells as described below. At least two different batches of chemerin isoforms were used for experiments.

Antimicrobial microdilution assay (MDA)

For antimicrobial experiments *E.coli* HB101 were grown in brain heart infusion (BHI) broth at 37°C. To determine the antimicrobial activity of the chemerin isoforms, bacteria in mid-logarithmic phase were harvested, washed three times with PBS and diluted to 4×10^5 CFU/ml with PBS. Then bacteria were incubated with either chemerin isoforms (3 μ M) or PBS (control) for 2 h. The number of viable bacteria were enumerated by CFU counting.

Chemotaxis assay

Purified mouse chemerin isoforms were tested for the ability to stimulate migration of the murine pre-B lymphoma cell line L1.2 stably transfected with mouse CMKLR1 (L1.2-CMKRL1). L1.2-CMKRL1+ cell were provided by Dr. Brian Zabel and Dr. Eugene C. Butcher (Stanford University School of Medicine and Veterans Affairs Palo Alto Health Care System). A total of 100 μ l cells (2×10^5 cells/well) was added to the top well of 5- μ m pore Corning Costar Transwell inserts (Corning, USA). Chemotaxis assay was performed in chemotaxis media (RPMI 1640 with 10% FBS) containing 1 nM of chemerin, added to the bottom well in a 600- μ l volume. Migration was assayed for 2 h at 37°C. The inserts were then removed, and cells that had migrated through the filter to the lower chamber were collected and counted by flow cytometry (LSRII; BD Biosciences, USA). The results are presented as percentage of input migration.

Statistical analysis

Differential splicing quantification from RNA-Seq experiments was performed using vast-tools (-r 0.95, and -m 0.1). Other data were analyzed using STATISTICA 13 (StatSoft, Tulsa, OK, USA). The results were visualized with Prism (GraphPad Software, San Diego, CA, USA), and presented as mean \pm standard deviation (SD). The Student's t-test was used for comparison between two groups. For multiple

comparisons, analysis of variance (ANOVA) with Tukey's post-hoc test was used. Differences were considered statistically significant for p-values of less than 0.05.

Declarations

Author contributions

K.K, J.C. and M.K. conceived and designed the experiments; K.K., P.M., P.B., U.G., and I.S. performed experiments; M.B. analyzed RNA-seq data, K.K., P.B., U.G., J.C. and M.K. analyzed data; M.K. wrote the manuscript. All authors have approved the manuscript.

Acknowledgments

This work was supported by the Polish National Science Center grants: UMO-2013/10/E/NZ6/00745 (to M.K.) and UMO 2014/12/W/NZ6/00454 (to J.C.). The open-access publication of this article was funded by the Priority Research Area BioS under the program "Excellence Initiative – Research University" at the Jagiellonian University in Krakow.

Competing interests

The authors declare that there are no competing interests associated with this manuscript to report.

References

1. Nilsen, T. W. & Graveley, B. R. Expansion of the eukaryotic proteome by alternative splicing. *Nature* (2010). doi:10.1038/nature08909
2. Gunning, P. W. Protein Isoforms and Isozymes. in *Encyclopedia of Life Sciences* (2006). doi:10.1038/npg.els.0005717
3. Stastna, M. & Van Eyk, J. E. Analysis of protein isoforms: Can we do it better? *Proteomics* (2012). doi:10.1002/pmic.201200161
4. Germain, C. *et al.* Characterization of alternatively spliced transcript variants of CLEC2D gene. *J. Biol. Chem.* (2010). doi:10.1074/jbc.M110.179622
5. Zabel, B. A. *et al.* Chemerin regulation and role in host defense. *Am. J. Clin. Exp. Immunol.***3**, 1–19 (2014).
6. Banas, M. *et al.* Chemerin Is an Antimicrobial Agent in Human Epidermis. *PLoS One***8**, 2–9 (2013).
7. Banas, M. *et al.* The expression and regulation of chemerin in the epidermis. *PLoS One***10**, 1–19 (2015).
8. Fagerberg, L. *et al.* Analysis of the human tissue-specific expression by genome-wide integration of transcriptomics and antibody-based proteomics. *Mol Cell Proteomics***13**, 397–406 (2014).

9. Zabel, B. A., Silverio, A. M. & Butcher, E. C. Chemokine-Like Receptor 1 Expression and Chemerin-Directed Chemotaxis Distinguish Plasmacytoid from Myeloid Dendritic Cells in Human Blood. *J. Immunol.***174**, 244–251 (2005).
10. Skrzeczyńska-Moncznik, J. *et al.* Chemerin and the recruitment of NK cells to diseased skin. *Acta Biochim. Pol.***56**, 355–360 (2009).
11. Zabel, B. A. *et al.* Chemokine-like receptor 1 expression by macrophages in vivo: Regulation by TGF- β and TLR ligands. *Exp. Hematol.***34**, 1106–1114 (2006).
12. Goralski, K. B. *et al.* Chemerin, a novel adipokine that regulates adipogenesis and adipocyte metabolism. *J. Biol. Chem.***282**, 28175–28188 (2007).
13. Wanninger, J. *et al.* Adiponectin upregulates hepatocyte CMKLR1 which is reduced in human fatty liver. *Mol. Cell. Endocrinol.***349**, 248–254 (2012).
14. Du, X. Y. & Leung, L. L. K. Proteolytic regulatory mechanism of chemerin bioactivity. *Acta Biochim. Biophys. Sin. (Shanghai)*. (2009). doi:10.1093/abbs/gmp091
15. Zabel, B. A. *et al.* Chemerin activation by serine proteases of the coagulation, fibrinolytic, and inflammatory cascades. *J. Biol. Chem.***280**, 34661–34666 (2005).
16. Huang, H. *et al.* Chemerin isoform analysis in human biofluids using an LC/MRM-MS-based targeted proteomics approach with stable isotope-labeled standard. *Anal. Chim. Acta* (2020). doi:10.1016/j.aca.2020.08.062
17. Guillabert, A. *et al.* Role of neutrophil proteinase 3 and mast cell chymase in chemerin proteolytic regulation. *J. Leukoc. Biol.* (2008). doi:10.1189/jlb.0508322
18. Zhao, L. *et al.* Chemerin158K protein is the dominant chemerin isoform in synovial and cerebrospinal fluids but not in plasma. *J. Biol. Chem.* (2011). doi:10.1074/jbc.M111.258954
19. Zhao, L., Yamaguchi, Y., Shen, W. J., Morser, J. & Leung, L. L. K. Dynamic and tissue-specific proteolytic processing of chemerin in obese mice. *PLoS One* (2018). doi:10.1371/journal.pone.0202780
20. NCBI. Available at: <https://www.ncbi.nlm.nih.gov/gene/71660>.
21. No Title. Available at: <https://www.ensembl.org/index.html>.
22. N.A., O. *et al.* Reference sequence (RefSeq) database at NCBI: Current status, taxonomic expansion, and functional annotation. *Nucleic Acids Res.* (2016).
23. Tapial, J. *et al.* An atlas of alternative splicing profiles and functional associations reveals new regulatory programs and genes that simultaneously express multiple major isoforms. *Genome Res.* (2017). doi:10.1101/gr.220962.117
24. Camacho Londoño, J. & Philipp, S. E. A reliable method for quantification of splice variants using RT-qPCR. *BMC Mol. Biol.* (2016). doi:10.1186/s12867-016-0060-1
25. Kwiecien, K. *et al.* The methylation status of the chemerin promoter region located from – 252 to + 258 bp regulates constitutive but not acute-phase cytokine-inducible chemerin expression levels. *Sci. Rep.* (2020). doi:10.1038/s41598-020-70625-7

26. Godlewska, U. *et al.* Bacteria Modify Their Sensitivity to Chemerin-Derived Peptides by Hindering Peptide Association With the Cell Surface and Peptide Oxidation. *Front. Microbiol.* (2020). doi:10.3389/fmicb.2020.01819
27. Buechler, C., Feder, S., Haberl, E. M. & Aslanidis, C. Chemerin isoforms and activity in obesity. *Int. J. Mol. Sci.***20**, (2019).
28. Feder, S., Bruckmann, A., McMullen, N., Sinal, C. J. & Buechler, C. Chemerin isoform-specific effects on hepatocyte migration and immune cell inflammation. *Int. J. Mol. Sci.* (2020). doi:10.3390/ijms21197205
29. Lareau, L. F., Green, R. E., Bhatnagar, R. S. & Brenner, S. E. The evolving roles of alternative splicing. *Current Opinion in Structural Biology* (2004). doi:10.1016/j.sbi.2004.05.002
30. Pan, Q., Shai, O., Lee, L. J., Frey, B. J. & Blencowe, B. J. Deep surveying of alternative splicing complexity in the human transcriptome by high-throughput sequencing. *Nat. Genet.* (2008). doi:10.1038/ng.259
31. Wang, E. T. *et al.* Alternative isoform regulation in human tissue transcriptomes. *Nature* (2008). doi:10.1038/nature07509
32. Tian, Y. *et al.* A novel splice variant of folate receptor 4 predominantly expressed in regulatory T cells. *BMC Immunol.* (2012). doi:10.1186/1471-2172-13-30
33. Rossner, P. *et al.* Inhalation of ZnO Nanoparticles: Splice Junction Expression and Alternative Splicing in Mice. *Toxicol. Sci.* (2019). doi:10.1093/toxsci/kfy288
34. Pachynski, R. K. *et al.* Chemerin Suppresses Breast Cancer Growth by Recruiting Immune Effector Cells Into the Tumor Microenvironment. *Front. Immunol.***10**, 983 (2019).
35. Niklowitz, P., Rothermel, J., Lass, N., Barth, A. & Reinehr, T. Link between chemerin, central obesity, and parameters of the Metabolic Syndrome: findings from a longitudinal study in obese children participating in a lifestyle intervention. *Int. J. Obes.***42**, 1743–1752 (2018).
36. Haberl, E. M. *et al.* Chemerin is induced in non-alcoholic fatty liver disease and hepatitis b-related hepatocellular carcinoma. *Cancers (Basel)*. (2020). doi:10.3390/cancers12102967
37. Parlee, S. D., Ernst, M. C., Muruganandan, S., Sinal, C. J. & Goralski, K. B. Serum chemerin levels vary with time of day and are modified by obesity and tumor necrosis factor- α . *Endocrinology***151**, 2590–2602 (2010).
38. Kwiecien, K. *et al.* Architecture of antimicrobial skin defense. *Cytokine and Growth Factor Reviews* (2019). doi:10.1016/j.cytogfr.2019.08.001
39. Chomczynski, P. & Sacchi, N. The single-step method of RNA isolation by acid guanidinium thiocyanate-phenol-chloroform extraction: Twenty-something years on. *Nat. Protoc.* (2006). doi:10.1038/nprot.2006.83
40. Livak, K. J. & Schmittgen, T. D. Analysis of relative gene expression data using real-time quantitative PCR and the 2- $\Delta\Delta$ CT method. *Methods***25**, 402–408 (2001).

41. Matsumura, I. & Bryksin, A. V. Overlap extension PCR cloning: a simple and reliable way to create recombinant plasmids. *Biotechniques* **48**, 463–465 (2010).

Figures

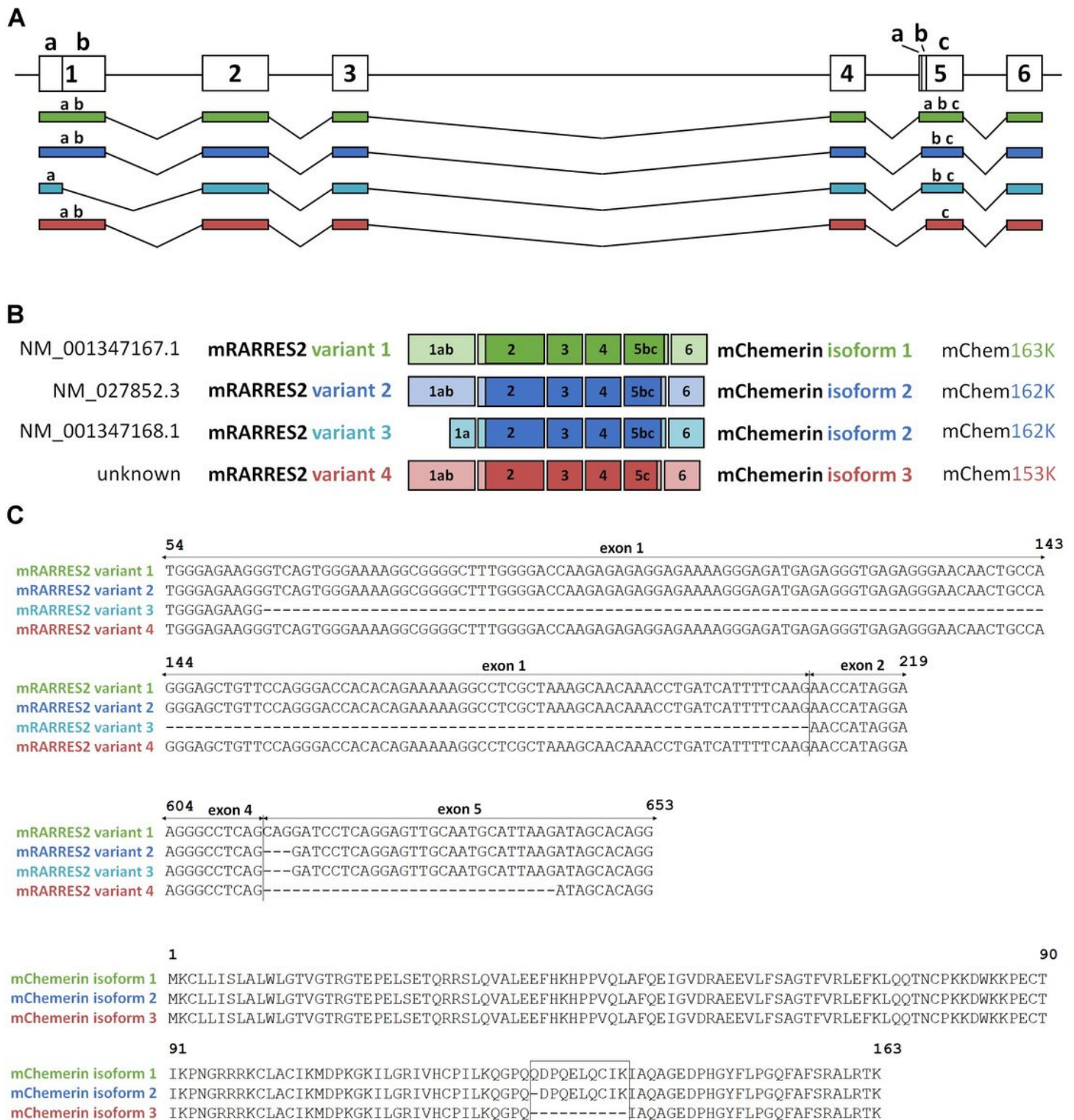


Figure 1

Schematic representation of RARRES2 alternatively spliced transcript variants. Schematic representation of RARRES2 transcript variants detected in mouse tissues using 3' and 5' RACE PCR (A). Alignment of nucleotide sequences of RARRES2 transcript variants (B). Alignment of predicted chemerin isoforms (C).

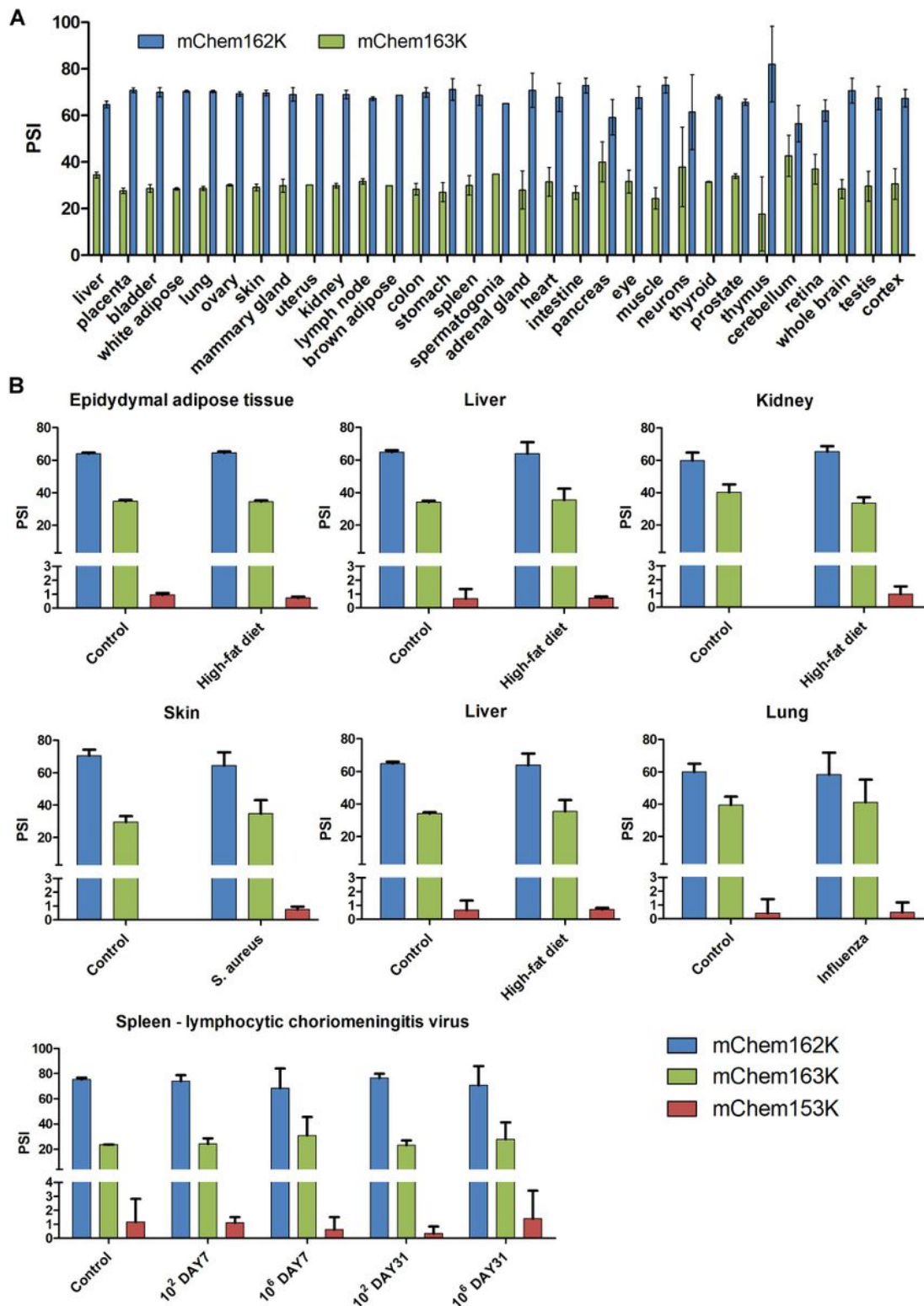


Figure 2

Analysis of RNA-seq experiments and VastDB database reveals tissue-wide expression of RARRES2 splice variants. Alternative splicing events of RARRES2 in distinct mouse tissues was acquired from

VastDB database (A). The effect of high-fat diet, *S. aureus*, *T. gondii*, influenza virus or lymphocytic choriomeningitis virus infection on RARRES2 splicing pattern was assessed using publicly available RNA-Seq datasets (B). The results are expressed as percent spliced-in (PSI) values. Differential splicing analyses using vast-tools did not reveal any statistically significant changes in splicing pattern between control and treatment groups.

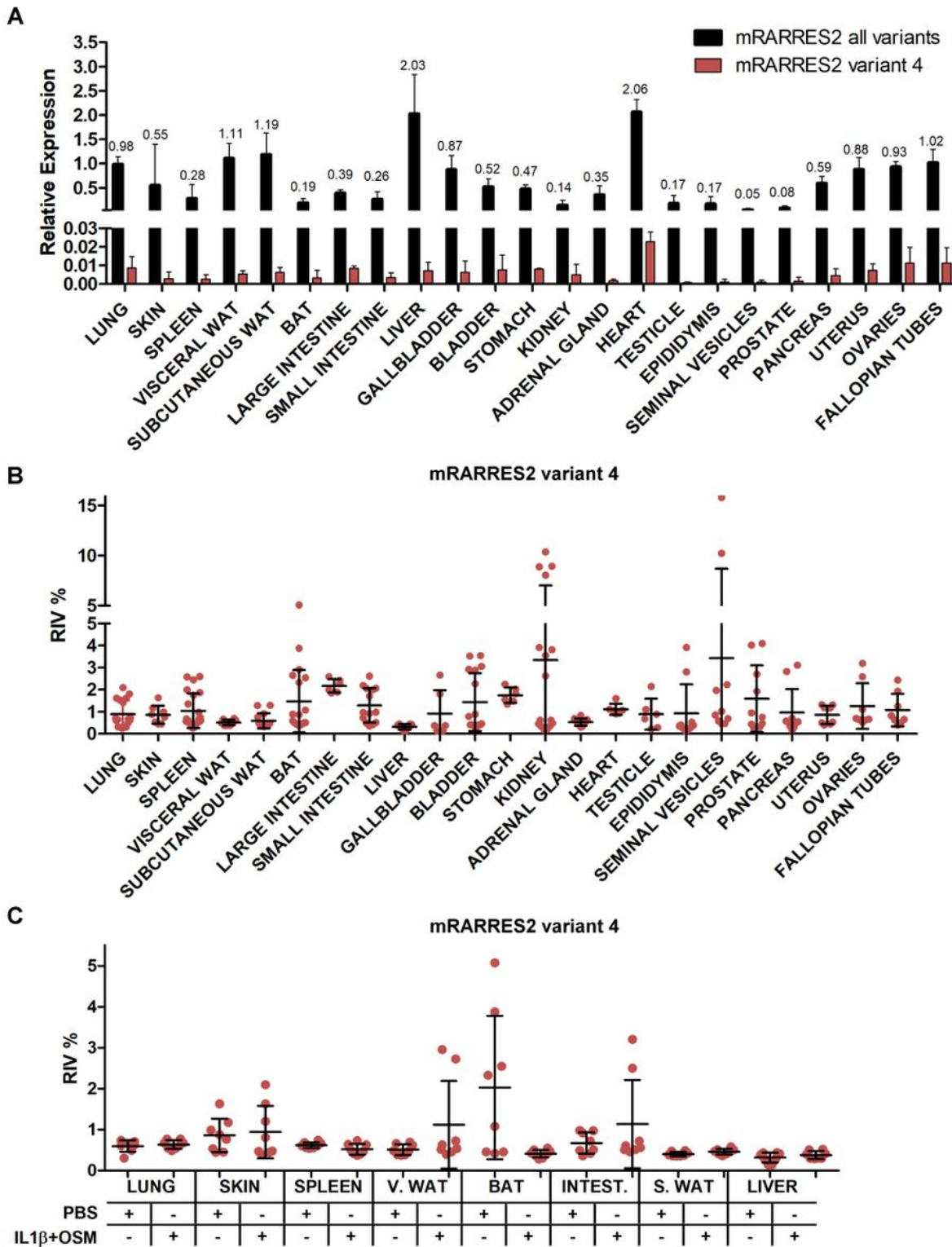
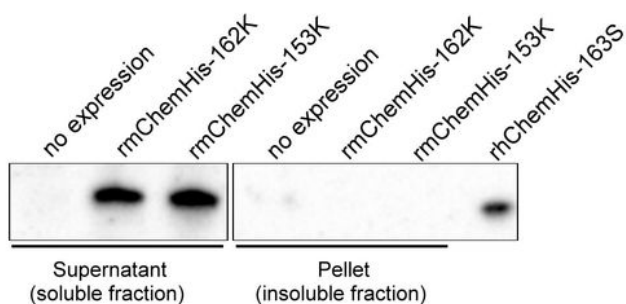
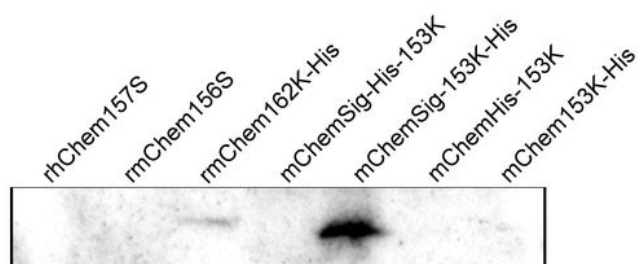
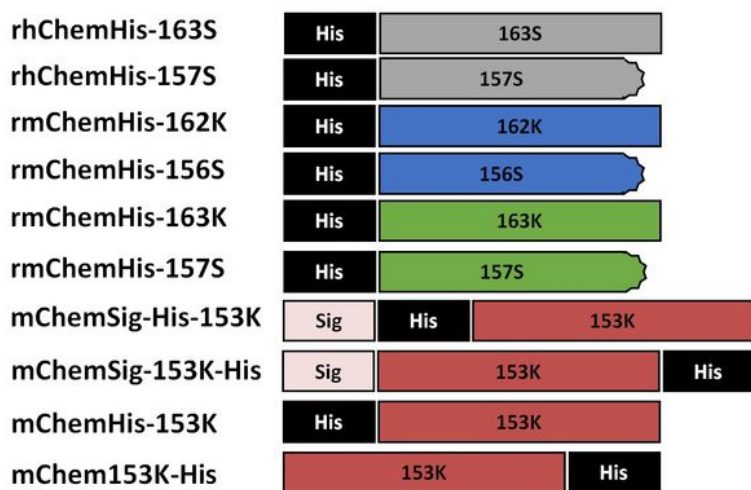


Figure 3

Acute-phase cytokines do not affect the relative incidence of RARRES2 variant 4 levels across distinct mouse tissues. In vivo, IL-1 β and OSM were injected intraperitoneally at doses of 10 μ g/kg BW and 160 μ g/kg BW, respectively. Control animals were treated with PBS. After 24 h, different tissues were isolated and subjected to RT-QPCR analysis. The levels of RARRES2 variant 4 in different organs and tissues of control animals is presented as relative expression values (A) or as relative incidence of variant (RIV) (B). The relative incidence of RARRES2 splice variant 4 in selected tissues of acute-phase cytokine or PBS treated animals is also shown (C). Data are presented as the mean \pm SD of at least three independent experiments. There were no statistically significant results between control and treatment groups; V. WAT – visceral white adipose tissue, S.WAT – subcutaneous white adipose tissue, INTEST. – intestine;

A**Expression of mChem153K in *E.coli*****B****Expression of mChem153K in HEK293****C****Schematic representation of chemerin isoforms expressed in *E.coli* and HEK293****Figure 4**

RARRES2 transcript variant 4 is translated into the protein. *E. coli* was transformed with the pNIC28-Bsa4 plasmids encoding mChem163K or mChem153K with N-terminal His-tag (His). Supernatant and pellet fractions from the *E. coli* culture were resolved by SDS-PAGE and immunoblotted with an anti-His-tag antibody. His-tagged recombinant human chemerin (rhChemHis-163S, 20 ng) was used as a control (A). HEK293 cells were transfected with the pcDNA plasmids coding for mChem153K with different

localizations of signal peptide (Sig) and His-tag (His). Cell lysates were subjected to western blot analysis as described above (B). Commercially available human (rhChem157S) and mouse (rmChem156S) recombinant chemerin lacking His-tag were used as negative control. His-tagged recombinant mouse chemerin (rmChem162K, 20 ng) was used as positive control. Schematic representation of chemerin isoforms used in the study is shown(C).

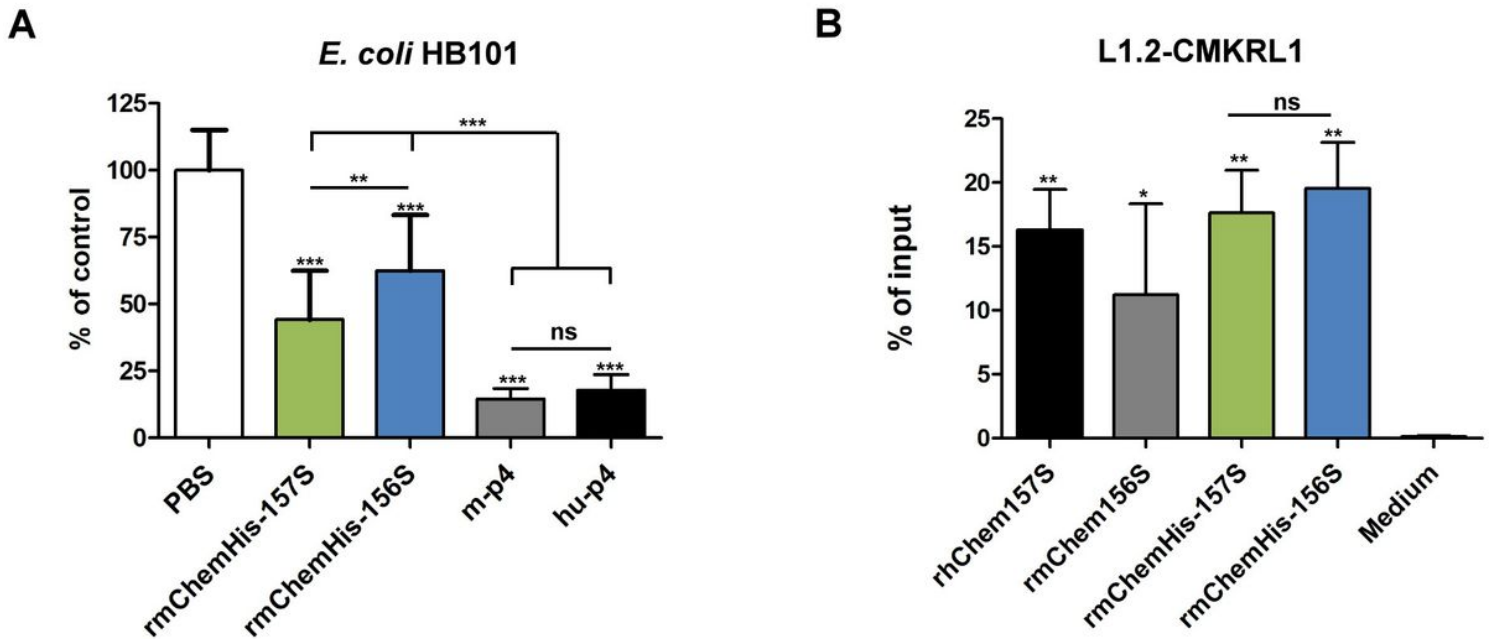


Figure 5

Chemerin isoform mChem157S exhibits higher bactericidal but not chemotactic activity compared to mChem156S. Bacteria were incubated with chemerin isoforms (3 μ M) lacking six terminal aa, PBS (negative control), human or mouse peptide p4 (positive control) for 2 h. Cell viability, shown as the percentage of a control cells, was analyzed by MDA assay (A). Chemotactic bioactivity of chemerin isoforms (1nM) was evaluated by in vitro transwell assay using CMKLR1 expressing L1.2 cells. Migration to bioactive recombinant rhChem157S and rmChem156S at 1nM, and chemotaxis medium is shown as a positive and negative control, respectively (B). Results are expressed as the mean \pm SD of at least three independent experiments using two different chemerin production batches. *** $p < 0.001$, ** $p < 0.01$, * $p < 0.05$ by one-way ANOVA with post-hoc: Tukey's multiple comparisons test.

Supplementary Files

This is a list of supplementary files associated with this preprint. Click to download.

- [SupplementaryScientificReports.docx](#)